Hindawi
Geofluids
Volume 2021, Article ID 6465193, 10 pages
https://doi.org/10.1155/2021/6465193

Research Article

Research on Organic Nanopore Adsorption Mechanism and Influencing Factors of Shale Oil Reservoirs

Yanfeng He,[1] Guodong Qi,[1] Xiangji Dou,[1] Run Duan,[1] Nan Pan,[1] Luyao Guo,[1] and Zhengwu Tao[2]

[1]*School of Petroleum Engineering, Changzhou University, Changzhou 213164, China*
[2]*PetroChina Tarim Oilfield Company, Kulle, Xinjiang 841000, China*

Correspondence should be addressed to Xiangji Dou; dxj@cczu.edu.cn

Received 21 October 2021; Accepted 16 November 2021; Published 1 December 2021

Academic Editor: Wei Yu

The adsorption properties of shale oil are of great significance to the development of shale oil resources. This study is aimed at understanding the microscopic adsorption mechanism of shale oil in organic nanopores. Thus, a molecular model of organic micropore walls and multicomponent fluids of CO_2, $C4H_{10}$, C_8H_{18}, and $C_{12}H_{26}$ is constructed to investigate the adsorption pattern of multicomponent fluids in organic nanopores under different temperature and pore size conditions. The quantity and heat of adsorption are simulated with the Monte Carlo method, which has been used in previous studies for single-or two-component fluids. The results demonstrate that the ability of CO_2 to displace various alkanes is different. Specifically, medium-chain n-alkanes are slightly weaker than light alkanes in competitive sorption, and long-chain n-alkanes are less conducive to competitive sorption. The higher the CO_2 sorption ratio, the more the sorption sites occupied by CO_2. Thus, it is the best replacement for shale oil. The adsorption quantity of carbon dioxide, n-butane, and n-octane in organic nanopores first increases and then decreases as temperature rises. Meanwhile, the adsorption quantity of n-dodecane decreases firstly and then increases. With the increase in the pore size, the adsorption quantity of carbon dioxide, n-butane, and n-octane in organic nanopores increases while the adsorption quantity of n-dodecane first increases and then decreases. Besides, the model with larger pore sizes is more sensitive to pressure changes in the adsorption of carbon dioxide and n-butane than the model with smaller pore sizes. The heat of adsorption is CO_2, $C_{12}H_{26}$, C_8H_{18}, and C_4H_{10} in descending order. All are physical adsorption. Moreover, the adsorption quantity of all four components mixed fluid in the organic matter nanopores is positively correlated with the heat of adsorption.

1. Introduction

With the increasing demand for energy sources and the gradual depletion of conventional oil and gas resources around the world, searching for another unconventional alternative energy source is an inevitable trend for future energy development. Shale oil is a typical unconventional oil and gas resource, an essential supplementary and alternative energy source. Thus, countries around the world are beginning to focus on shale oil exploration and extraction. Generally, most shale oil in an adsorbed or free state is stored in the shale, and a small amount of shale oil keeps a dissolved (or miscible) state [1–3]. The characteristics of shale oil stored in shale reservoirs with low porosity and low permeability make it more difficult to exploit shale oil. Therefore, it is necessary to explore the adsorption and desorption of shale oil in organic nanopores. Its laws will provide theoretical guidance for shale oil extraction [4]. In recent years, molecular dynamic simulation techniques have presented great potential for quantitative characterization of adsorption resolution, interactions, and fluid transport in nanomaterials. They have been gradually introduced into petroleum research. Shale oil possesses a higher alkane content compared with conventional crude oil. However, it is a typical multicomponent fluid whose component composition is extremely complex [5]. Typically, shale oil under stratigraphic conditions may contain short-chain n-alkanes (such as methane CH_4), medium-chain n-alkanes (such as

n-hexane n-C_6H_{14}), and long-chain n-alkanes (such as n-dodecane n-$C_{12}H_{26}$), which are generally stored in organic nanopores in an adsorbed or free state. Shale oil is mainly composed of hydrocarbons, sulphur-containing compounds, nitrogen-containing compounds, etc. From the microscopic mechanism point of view, n-$C_{12}H_{26}$, as the main compound component of the oil phase of shale oil, can be a good substitute for shale oil at the nanoscale to simulate the competitive sorption of CO_2 and shale oil. As the pore size of shale parent material is in the nanometer range, the permeability coefficient of shale oil in shale parent material is extremely small. Besides, the macroscopic flow mechanism does not apply to the flow pattern of shale oil in the shale parent material [6, 7]. Therefore, it significantly increases the difficulty of studying the adsorption and desorption of shale oil in nanopores.

The sorption and desorption of shale gas in organic and in organic nanopores have been extensively studied by many researchers [8–10], while there are few studies on the sorption and desorption of shale oil in organic and inorganic nanopores [11, 12]. Pathank et al. [13] discovered that carbon dioxide can effectively replace shale gas adsorbed in shale cheesecake by investigating the adsorption-desorption law of methane and carbon dioxide in the three systems of methane-carbon dioxide-kerogen. Wu and Liu [14] employed the GCMC method to simulate the effects of temperature, pressure, and gas molar fraction on the adsorption and separation of CO/H_2 mixture in carbon nanopores and obtained the optimal pore width for the separation of CO/H_2. Zhou et al. [15] explored the effects of reservoir temperature, pressure conditions, and the molar fraction of CO_2 in the CO_2/CH_4 gas mixture on the separation of CO_2/CH_4 in slit-type pores in coal seams with the GCMC method. With the increase in pressure, the equilibrium separation coefficient of CO_2 relative to CH_4, SCO_2/CH_4, initially increases until it reaches the peak, then decreases, and lastly tends to be constant at 20 MPa. Besides, Chen et al. [16] discovered the adsorption characteristics of CH_4 and C_2H_6 on illite at high-temperature conditions (60°C, 90°C, and 120°C) by Monte Carlo method, revealing that the main influencing factor of CH_4 and C_2H_6 adsorption is the layer spacing, and the excess adsorption of C_2H_6 is twice as much as that of CH_4 at layer spacing above 2 nm. Wang et al. [17] investigated the storage pattern of straight-chain alkanes in slit pores formed by organic matter through molecular dynamics simulations, concluding that multiple alkane adsorption layers existed on the slit pore surface whose layer thickness is approximately 0.42 nm. Moreover, Wang [18] established an initial model of $scCO_2$ repelling shale oil in rock pores and performed the kinetic simulations to observe the microconfiguration diagrams of the oil repelling process and qualitatively analyze the mechanism of $scCO_2$ oil repelling. They revealed the microaction mechanism of $scCO_2$ repelling shale oil. Most of the shale oil adsorption simulation studies were conducted with two components. There are few simulation experiments for exploring the adsorption and desorption of multicomponent fluids such as CO_2/CH_4/C_2H_6 and some polymeric alkanes under reservoir conditions. Many researchers have investigated the effects of temperature and pore size and other conditions on the adsorption and desorption of shale gas in organic nanopores and inorganic nanopores. However, the effect of temperature, pore size, component ratio, and other conditions on the adsorption of organic nanopores in shale oil reservoirs is rarely studied.

Therefore, the Grand Canonical Monte Carlo (GCMC) and Molecular Dynamic (MD) methods are employed to research the effect of different molar ratios of CO_2, C_4H_{10}, C_8H_{18}, and $C_{12}H_{26}$ on the competitive adsorption pattern of each component with molecular dynamic simulations to address the above issues. The effect of formation temperature on the adsorption of multicomponent fluids composed of CO_2, C_4H_{10}, C_8H_{18}, and $C_{12}H_{26}$ in organic nanopores was investigated using the controlled variable method with the same formation pressure and the unchanged pore space, at various temperatures of the formation [19]. Under the same conditions of formation temperature and formation pressure, the size of organic nanopores in shale reservoirs was exchanged to explore the effect of the adsorption of multicomponent fluids in organic nanopores, so as to analyze the influence of changes of organic nanopores in shale oil reservoirs on the adsorption mechanism of shale reservoirs.

2. Simulation System

2.1. Construction of the Molecular Model. Graphite is a three-dimensional structure, which was composed of carbon atoms. The first step to be taken in this paper is to select the graphene single cell structure from the Materials Studio database. Then, the single-layer graphene structure is constructed using the build window of the software, and the graphene slit model is established by the build layer under the Visualizer task module. The vacuum layer between the two graphene sheets is the pore space. Its thickness of 20 Å, 40 Å, and 60 Å is taken to build a $15a \times 10b \times c$ supercell graphene structure model, respectively. The X and Y directions are set as a periodic structure while a, b, α, and β are fixed to repeatedly meet on infinite space to simulate the macroscopic system, as illustrated in Figure 1. CO_2, C_4H_{10}, C_8H_{18}, and $C_{12}H_{26}$ fluid molecular models are constructed by the Visualizer task module. Figure 2 presents the model of each component fluid, where (a) is the carbon dioxide molecular model, (b) is the n-butane molecular model, (c) is the n-octane molecular model, and (d) is the n-dodecane molecular model.

2.2. Optimization of the Calculation Model. The graphene structural model and the CO_2, C_4H_{10}, C_8H_{18}, and $C_{12}H_{26}$ molecular models need to be structurally optimized before the adsorption simulations of the molecules, so as to reach the lowest point of potential energy, that is, energy minimization. The resulting optimized models are used for molecular simulations. Firstly, the geometry of the constructed models was optimized by selecting the smart option in the task Geometry Optimization under the Molecular Dynamics Forcite module to obtain a stable graphene slit structure. Afterward, the COMPASS force field was selected for the force field; the atom-based summation method was used for the van der Waals forces; the rest of the settings were

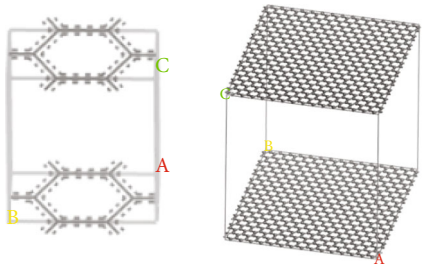

Figure 1: Organic matter pore model.

kept as the software defaults. The fluid models of CO_2, C_4H_{10}, C_8H_{18}, and $C_{12}H_{26}$ were optimized in the same way Error! Reference source not found [20]. This is exhibited in Figure 2.

2.3. Potential Energy Model. In this paper, the simulations of CO_2, C_4H_{10}, C_8H_{18}, $C_{12}H_{26}$, and the C atoms in the graphite layer and the molecule-molecule interactions are performed for the L-J potential energy model [21], whose specific parameters are provided in Table 1. The van der Waals forces between the covalently bonded molecules in the system are described by the potential energy function:

$$U(ij) = 4\varepsilon_{ij}\left[\left(\frac{\sigma_{ij}}{r_{ij}}\right)^{12} - \left(\frac{\sigma_{ij}}{r_{ij}}\right)^{6}\right] + \frac{qq^{ji}}{r_{ij}}, \quad (1)$$

where: r_{ij} is the distance between particles i and j, q_i is the charged quantity of particle i, q_j is the charged quantity of particle j, ε_{ij} is the energy action parameter, and σ_{ij} is the dimensional action parameter;

2.4. Simulation Program. The adsorption processes of carbon dioxide, n-butane, n-octane, and n-dodecane in organic matter nanopores were simulated to investigate the effects of different pore sizes, different temperatures, and different molar ratios of different fluids on the adsorption capacity of carbon dioxide, n-butane, n-octane, and n-dodecane in organic matter nanopores. The components of fluids were carbon dioxide, n-butane, n-octane, and n-dodecane in molar ratios of 1 : 1 : 1 : 1, 4 : 1 : 1 : 1, and 1 : 4 : 1:1 to simulate the competing adsorption patterns of different molar ratios of the different components in the organic nanopores, respectively [22]. The simulated pore sizes range from 10 Å to 60 Å, and the simulated temperatures range from 333 K to 433 K. The default temperature in all simulation scenarios is 373 K, the pore sizes are 40 Å, and the pressures are 0-30 MPa, except for the temperature mechanism effect, which is divided into 11 pressure points. Besides, the simulations are developed separately.

The simulations are detailed as follows. Periodic boundary conditions are set in the X and Y directions of the organic nanopores. The COMPASS force field is used for all calculations. Besides, the NVT system is used. It is a system in which the atomic number N, volume V, and temperature T are constants. The calculation is conducted using the Fix Pressure task under the Sorption module. The total number of production steps is 100,000, of which 10,000 are equilibration steps. The parameters such as van der Waals force, cut-off radius, and key tooth width are set as the same as those used in the structural optimization.

3. Study of Competitive Adsorption Patterns

3.1. Competitive Adsorption Laws for the Same Molar Ratio. The main component of shale oil contains some long-chain n-alkanes. Currently, a large number of studies have been conducted to enhance the recovery of shale oil by injecting carbon dioxide into the shale reservoir. Since different types of fluids have different adsorption capacities, the grand canonical Monte Carlo method is used to simulate the competitive adsorption of multicomponent mixed fluids with the same molar ratio in the pores of organic shale. The competing sorption patterns of carbon dioxide, n-butane, n-octane, and n-dodecane in organic nanopores were explained from a microscopic perspective. Besides, the competitive adsorption of a mixture of carbon dioxide, n-butane, n-octane, and n-dodecane in the same molar ratio (carbon dioxide : n – butane : n – octane : n – dodecane = 1 : 1 : 1 : 1) in organic nanopores with a pore size of 40 Å was simulated at 373 K. The adsorption quantity of the multicomponent fluids was obtained for pressure variations from 1 to 30 MPa. The adsorption isotherm curves for a molar ratio of 1 : 1 : 1 : 1 are illustrated in Figure 3. Additionally, the adsorption configuration for a multicomponent fluid mixed with the same molar ratio is exhibited in Figure 4.

As observed in Figure 3, the adsorption of carbon dioxide, n-butane, n-octane, and n- dodecane in the pores of organic matter all rapidly increased with pressure before the low-pressure stage, followed by a slow rise. The four fluids reached saturation at approximately 10 MPa, and carbon dioxide reached saturation before n-butane, n-octane, and n-dodecane [23]. The sorption of carbon dioxide is approximately five times greater than that of n-butane while the difference in sorption between n-octane and n-dodecane is not significant, with n-octane slightly higher than n-dodecane. There was a significant reduction in the adsorption of the three-component fluids compared to the adsorption of n-butane, n-octane, and n-dodecane as single components in the pores of the organic matter.

The adsorption configuration diagram demonstrates a clear adsorption layer on the organic wall. Besides, the adsorption pattern of different components of the fluid on the organic wall is different, reflecting that CO_2 has different abilities to displace various types of alkanes [24, 25]. A large number of long-chain n-alkanes were adsorbed on the graphene wall, such as CO_2 and n-butane. Regarding the medium-chain n-alkanes, n-octane (green in the adsorption configuration diagram) is more apparently adsorbed in aggregates on the organic wall. Due to the strength of the adsorption capacity, the medium-chain n-alkanes are slightly weaker than the light alkanes in competitive adsorption. Moreover, most of the adsorption sites on the organic wall are occupied by CO_2 and n-butane. The competitive adsorption capacity of long-chain n-alkanes is the weakest,

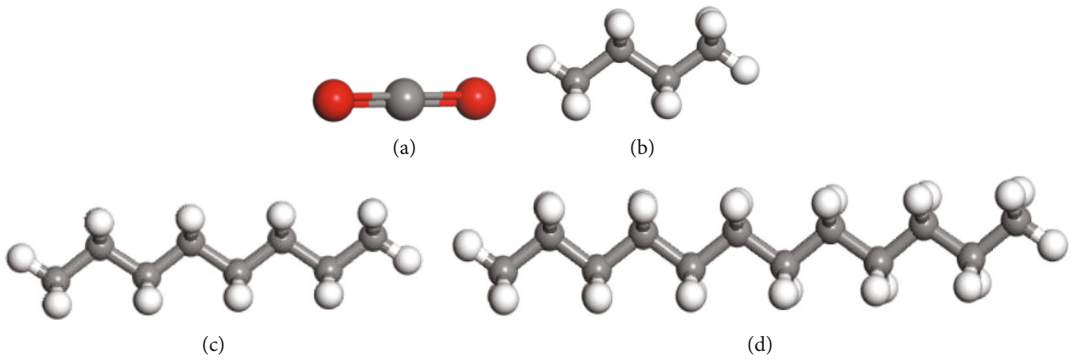

Figure 2: Fluid molecular model.

Table 1: *L-J* potential energy parameter table.

Site	σ/nm	(ε/K_B)/K
CO_2	0.363	242.0
C(CNT)	0.350	35.26
C_4H_{10}	0.525	350.5
C_8H_{18}	0.652	594.0
$C_{12}H_{26}$	0.785	715

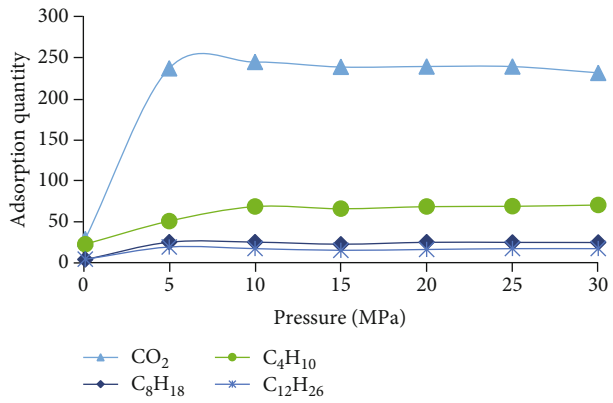

Figure 3: Isothermal adsorption curves for mixed fluid components of 1 : 1 : 1 : 1.

and the adsorption quantities are the smallest among the multicomponent fluids. This reveals that long-chain n-alkanes are not conducive to competitive adsorption while shale oil is composed mostly of medium-chain and long-chain n-alkanes. Additionally, it is extremely difficult to develop shale oil. Therefore, this multicomponent competitive adsorption model well explains the competitive adsorption law of CO_2, n-butane, n-octane, and n-dodecane in organic nanopores at the microscopic level. Experimental studies of shale oil are limited by the difficulty of observing the microscopic processes of CO_2-repelled shale oil, and the microscopic mechanisms of CO_2-repelled shale oil in nanopores are unclear. Therefore, it is important to simulate the process of CO_2 repelling shale oil through the competitive adsorption between CO_2 and multicomponent to achieve the guidance of studying the microscopic mechanism of CO_2 repelling shale oil in nanopores, and this has important practical significance to guide the CO_2 extraction of shale oil.

3.2. Competitive Adsorption Patterns for Different Molar Ratios. The competing adsorption of mixed component fluids of carbon dioxide, n-butane, n-octane, and n-dodecane in four different molar ratios (carbon dioxide : n – butane : n – octane : n – dodecane = 4 : 1 : 1 : 1, 1 : 4 : 1, 1 : 1 : 4 : 1 and 1 : 1 : 1 : 4) in organic matter nanopores with a pore size of 40 Å was simulated using the Monte Carlo method. Adsorption ratio curves were obtained for multicomponent fluids at pressure variations from 1 to 30 MPa. The simulated temperature was 373 K, and the simulated pressure was 0.1-30 MPa. Figures 5–7 exhibit the adsorption ratio curves of carbon dioxide and n-butane, carbon dioxide and n-octane, and carbon dioxide and n-dodecane, respectively.

These curves demonstrate that the sorption ratios of carbon dioxide to n-butane, n-octane, and n-dodecane all first increase and then tend to equilibrate. Overall, the increase in the adsorption ratio indicates that carbon dioxide consistently occupies more adsorption sites in competition with n-butane, n-octane, and n-dodecane in the adsorption process. The larger the proportion of carbon dioxide in the fluid mixture, the more the adsorption sites occupied by carbon dioxide and the relatively less the n-butane, n-octane, and n-dodecane adsorbed in the organic matter pores. The effect of the different ratios of molarity on the adsorption ratio is still significant. As reflected from the adsorption ratio curves, the adsorption ratios of carbon dioxide to n-butane, n-octane, and n-dodecane mixed ratios are 4 : 1, 1 : 1, and 1 : 4, respectively. The adsorption ratio when carbon dioxide is 4 molar ratio is greater than the adsorption ratio when n-butane, n-octane, and n-dodecane are 4 molar ratio to 1 molar ratio. This indicates that the higher the carbon dioxide adsorption ratio, the more carbon dioxide. Moreover, the replacement effect on shale oil is best and contributes more to significant CO_2 sequestration. Simultaneously, the ability of adsorption of crude oil itself is different under stratigraphic conditions owing to different components. The magnitude of the sorption ratio of CO_2 to n-butane, n-octane, and n-dodecane reflects the sorption rate of each component. Furthermore, the 4 : 1 mixture of CO_2 to n-butane, n-octane, and n-dodecane leads to a large difference

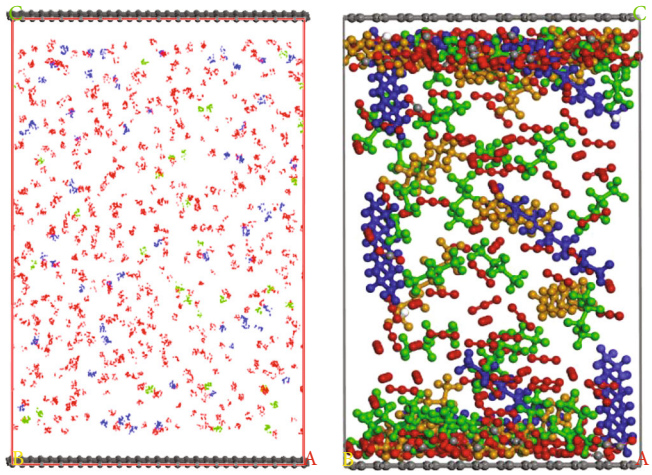

Figure 4: Adsorption configurations for mixed fluid components of 1 : 1 : 1:1.

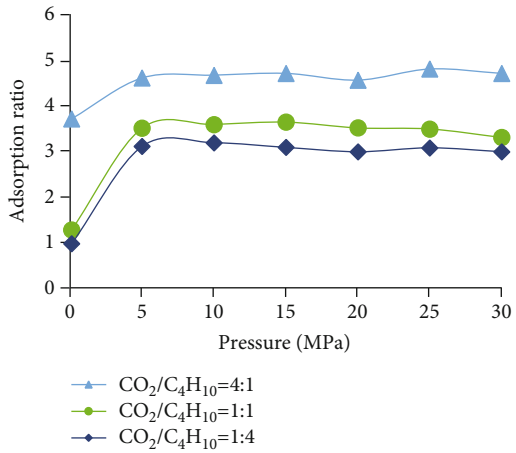

Figure 5: Carbon dioxide to n-butane adsorption ratio curve.

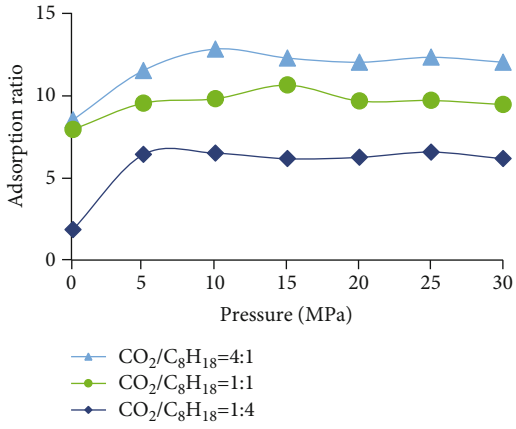

Figure 6: Carbon dioxide to n-octane adsorption ratio curve.

in sorption between the components. This implies that the replacement capacity of CO_2 for the different components is not the same [26].

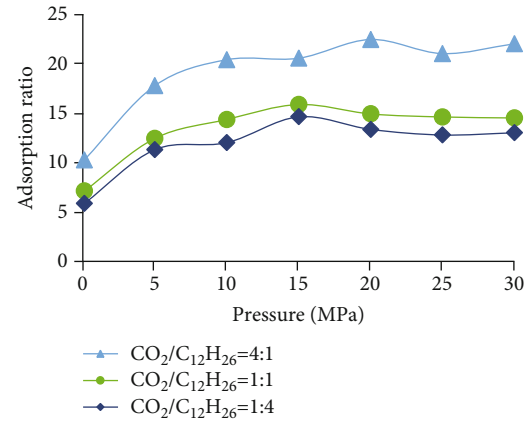

Figure 7: Carbon dioxide to n-dodecane adsorption ratio curve.

4. Effect of Temperature on Competitive Adsorption

The effect of temperature on the adsorption of multicomponent fluid mixtures was investigated with the adsorption quantity and adsorption configurations of carbon dioxide [27], n-butane, n-octane, and n-dodecane in organic matter nanopores at a mixture ratio of 1 : 1 : 1 : 1 as an example. The simulated temperature interval is 333-433 K, the pore width is 40 Å, and the simulated pressure is 0.1-30 MPa. The giant regular Monte Carlo method is employed for simulation. The isothermal adsorption curves of carbon dioxide, n-butane, n-octane, and n-dodecane under different temperature conditions are presented in Figures 8–11, respectively.

As indicated in the graph above, the adsorption quantity of carbon dioxide, n-butane, and n-octane in the organic nanopores of the multicomponent fluids first increases and then decreases with temperature, reaching a maximum for all three components at 373 K. As the temperature increases, the adsorption quantity decreases because the increase in temperature and pressure at the beginning of the simulation causes n-butane to add more kinetic energy and move more vigorously. Meanwhile, the chance of collision between

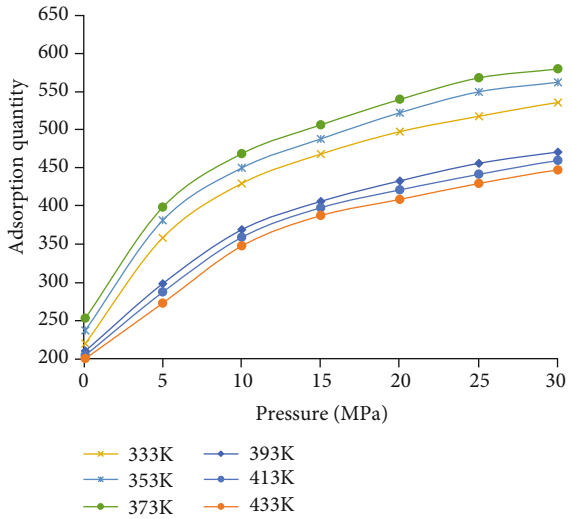

Figure 8: Isothermal adsorption curves for carbon dioxide at different temperatures.

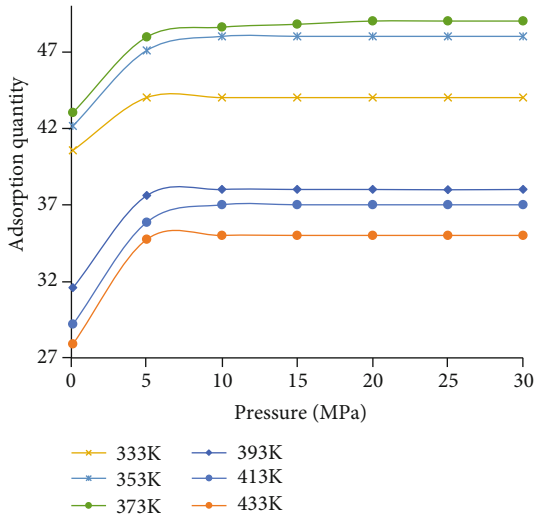

Figure 9: Isothermal adsorption curves for n-butane at different temperatures.

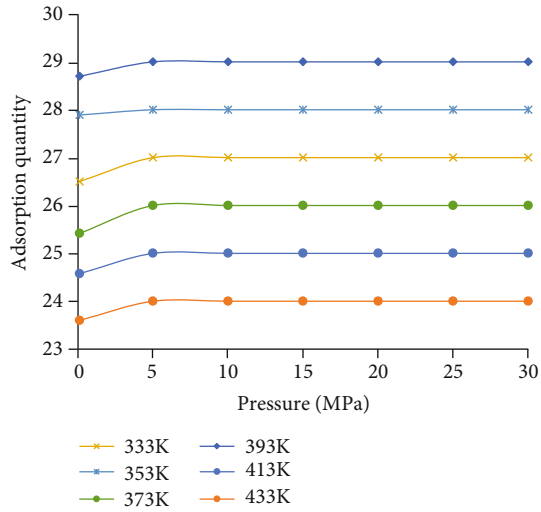

Figure 10: Isothermal adsorption curves for n-octane at different temperatures.

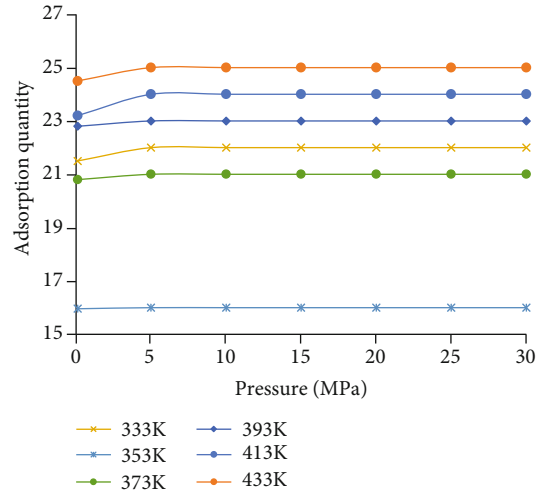

Figure 11: Isothermal adsorption curves for n-dodecane at different temperatures.

carbon dioxide, n-butane, n-octane, and organic matter nanopore walls increases, as well as the adsorption quantity. As the temperature and pressure continue to increase, the n-butane molecules gain more kinetic energy and thus tend to adsorb away from the organic nanopore structure, and the adsorption volume decreases.

The temperature-dependent adsorption pattern of n-dodecane in organic matter nanopores is opposite to that of carbon dioxide, n-butane, and n-octane. Figures 4 and 5 reveals that the amount of n-dodecane adsorbed first decreases and then increases with increasing temperature, and the maximum adsorption of n-dodecane was discovered at a temperature of 433 K, ascribed to the competition between the multicomponent mixture of carbon dioxide, n-butane, and n-octane. As the temperature increased to 373 K, the molecular movement of carbon dioxide, n-butane, and n-octane intensified, and the adsorption quantity reached its maximum [28]. When the temperature reaches 373 K, n-dodecane as a long-chain n-alkane does not intensify the movement of n-dodecane molecules, and the chance of collision between n-dodecane and organic matter nanopore walls does not increase, contributing to the reduction of adsorption quantity. Therefore, the maximum adsorption quantity of n-dodecane was achieved at a temperature of 433 K.

The temperature dependence of the adsorption of the mixed fluids competing for adsorption in the organic nanopores can be compared with that of the single-component fluids, demonstrating that the effect of temperature on the adsorption of the multicomponent fluids in the organic nanopores is weaker than that in the pure components n-butane, n-octane, and n-dodecane.

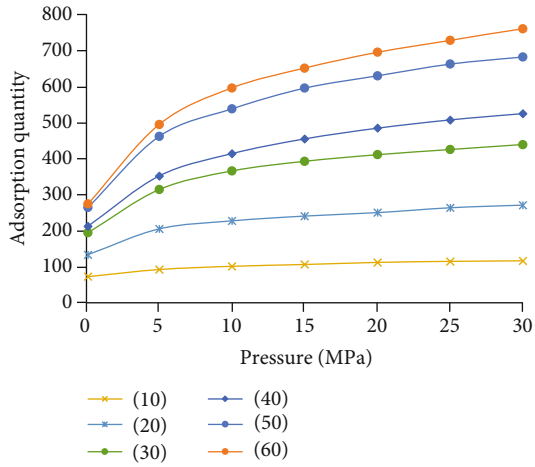

Figure 12: Isothermal adsorption lines for carbon dioxide at different pore sizes.

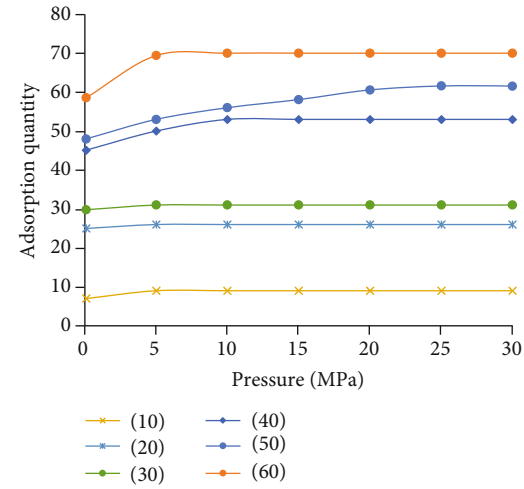

Figure 13: Isothermal adsorption curves for n-butane at different pore sizes.

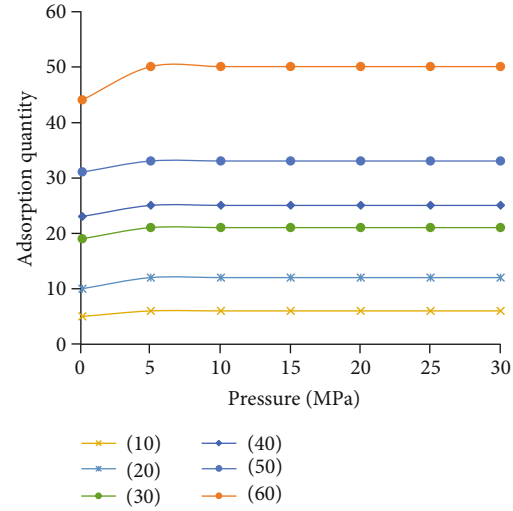

Figure 14: Isothermal adsorption lines for n-octane at different pore sizes.

As revealed from the graph above, the sorption ratios of carbon dioxide to n-butane, n-octane, and n-dodecane all tend to first increase and then decrease with the increasing temperature increases. The ratio eventually stabilizes. This can be explained that n-butane is a long-chain alkane, and molecular movement is more intense when the temperature increases. The sorption ratio of carbon dioxide to n-dodecane was less affected by temperature, and the effect of temperature change on n-dodecane in the fluid mixture was negligible. This suggests that short-chain alkanes are more susceptible to temperature influence compared to long-chain alkanes, and high temperature is more conducive to the desorption of alkanes and more beneficial to the replacement effect of shale oil.

5. Effect of Pore Size on Competitive Adsorption

The effect of pore size on the adsorption of multicomponent fluid mixtures was investigated by analyzing the adsorption and adsorption configurations in the nanopores of organic matter under a 1 : 1 : 1 : 1 mixture ratio of carbon dioxide, n-butane, n-octane, and n-dodecane [29]. The majority of shale oil storage environments are found in shale mesopores ranging in size from approximately 10 Å to 60 Å, which contains three intervals of pore size, including micropore, mesopore and macropore, and the range of pores in this interval allows for effective analysis of the effect of pore size on organic nanopore adsorption in shale reservoirs. The isothermal adsorption curves of carbon dioxide, n-butane, n-octane, and n-dodecane under different pore sizes are provided in Figures 12–15, respectively. Figures 16 and 17 present the adsorption configurations for pore sizes of 10 Å and 60 Å, respectively.

As indicated in Figures 12–15, the adsorption of carbon dioxide, n-butane, and n-octane in multicomponent fluids in the organic matter pore model at six pore sizes from smallest to largest is 10 Å, 20 Å, 30 Å, 40 Å, 50 Å, and60 Å. This implies that the adsorption of carbon dioxide, n-butane, and n-octane by organic matter nanopores increases with the increase in pore size. However, the adsorption quantity of n-dodecane in multicomponent fluids in six pore sizes of organic matter pore models from smallest to largest is 10 Å, 60 Å, 50 Å, 40 Å, 30 Å, and 20 Å. The adsorption quantity of n-dodecane first increased and then decreased with the increasing pore size. Besides, the pore size had a greater influence on the adsorption of fluids in the organic structure. The variation of carbon dioxide, n-butane, and n-octane adsorption with temperature and pressure is the smallest in the 10 Å organic matter nanopore model. The variation of carbon dioxide, n-butane, and n-octane adsorption with temperature and pressure is the largest in the 60 Å organic matter nanopore model. Thus, it can be assumed that competitive adsorption has no greater effect on the increase in the adsorption quantity of carbon dioxide, n-butane, and n-octane with the increasing pore size.

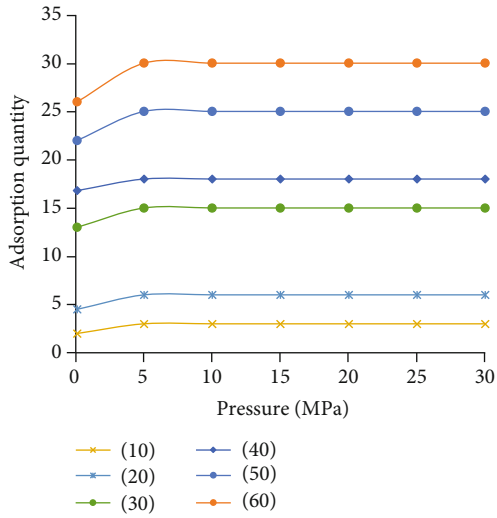

Figure 15: Isothermal adsorption curves for n-dodecane at different pore sizes.

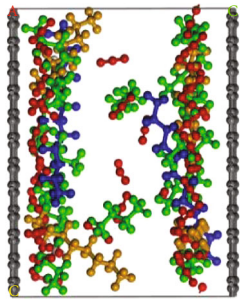

Figure 16: Adsorption configuration for a 10 Å pore size.

It can be concluded that the model with larger pore size has a greater effect on the adsorption quantity of carbon dioxide, n-butane, and n-octane than the model with smaller pore size in the adsorption quantity of carbon dioxide, n-butane, and n-octane adsorbed that is more sensitive to pressure changes [30]. The pore size was in the range of 20 Å ~40 Å when the pore size was a large variation in the adsorption of n-dodecane. It can be hypothesized that the competitive adsorption of long-chain alkanes in multicomponent fluids is gainful at 20 Å ~30 Å of organic matter nanopores, and the smaller pore size models are more sensitive to pressure changes in the adsorption of n-dodecane than the larger pore size models.

The graph of Figure 18 suggests that the sorption ratio of carbon dioxide to n-butane, n-octane, and n-dodecane in the mixed fraction significantly decreases as the pore size increases. The sorption ratio of carbon dioxide to n-butane changes most significantly, which has a small increase in pore size from 10 Å to 20 Å, a significant decrease in the section from 20 Å to 30 Å and then a steady decrease. The adsorption ratio of n-octane and n-dodecane decreases gradually with increasing pore size, and there is no process of increasing the adsorption ratio first, which is quite different from n-butane. As the adsorption ratio decreases, the

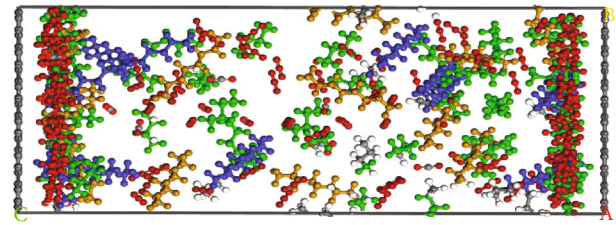

Figure 17: Adsorption configuration for a 60 Å pore size.

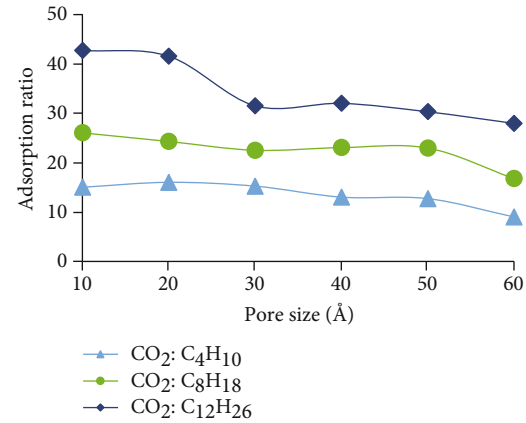

Figure 18: Adsorption ratio of methane to each component at different temperatures.

decrease in carbon dioxide sorption sites increases in n-butane, n-octane, and n-dodecane sorption sites. Therefore, the larger the pore size, the lower the sorption ratio, the more favorable the competition between carbon dioxide and the multicomponent fluid adsorption, and the more favorable to CO_2 replacement of shale oil in shale storage [31].

6. Heat of Absorption

The heat of adsorption is the heat released by the adsorption of adsorbent molecules on the adsorbent. It is an essential thermodynamic property of the adsorption process, which reflects the adsorption capacity of the adsorbent on the adsorbent and the nature of adsorption. The heat of adsorption is a crucial thermodynamic parameter distinguishing chemisorption from physical adsorption. The heat of adsorption is greater than 42 kJ/mol for chemisorption and less than 42 kJ/mol for physical adsorption [32]. Simultaneously, Figure 19 illustrates the molecular simulation of the heat of adsorption with pressure and temperature for the same proportion of a mixture of carbon dioxide, n-butane, n-octane, and n-dodecane in organic nanopores at a pore size width of 40 Å, a temperature of 333-433 K, and pressure of 10 MPa.

The graph above indicates that the heat of adsorption is CO_2, $C_{12}H_{26}$, C_8H_{18}, and C_4H_{10} in descending order. The heat of adsorption of carbon dioxide, n-butane, n-octane, and n-dodecane by organic nanopores is less than 42 kJ/

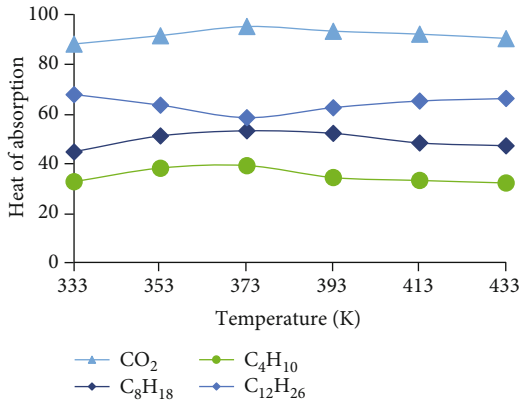

Figure 19: Variation curve of heat of adsorption with temperature.

mol, which is physical adsorption. The equivalent heat of adsorption of carbon dioxide, n-butane, n-octane, and n-dodecane increases with the increasing pressure at the same temperature. The equivalent heat of adsorption of n-dodecane first decreases and then increases as the temperature increases. It is positively correlated with the amount of n-dodecane mixed component fluid adsorbed in the organic matter nanopores. Carbon dioxide, n-butane, and n-octane all first increase and then decrease in the equivalent heat of adsorption with the increasing temperature. This is positively associated with the amount of carbon dioxide, n-butane, and n-octane adsorbed in the organic nanopores, that is in that the increase in temperature leads to an increase in the kinetic energy of carbon dioxide, n-butane, and n-octane seeds, making it easier for them to escape from the surface of the organic nanopore model, resulting in a decrease in the heat of adsorption.

7. Conclusion

(1) In simulations of competitive adsorption of the same molar ratios of CO_2, n-butane, n-octane, and n-dodecane, the adsorption patterns of the different components of the fluids on the pore surfaces of the organic matter and the ability of CO_2 to displace the various alkanes were different. Medium-chain alkanes are slightly weaker than short-chain alkanes in competitive adsorption while long-chain alkanes are less favorable to competitive adsorption

(2) In the multicomponent fluid competition adsorption law, the adsorption quantity of each component in the pores of organic matter increases with pressure. Besides, the adsorption quantity changes significantly when each component is adsorbed due to the different molar ratios. The sorption ratio of carbon dioxide at 4 molar ratios is greater than that of n-butane, n-octane, and n-dodecane at 4 molar ratios versus 1 molar ratio. This demonstrates that the higher the carbon dioxide sorption ratio, the more the carbon dioxide present, and the more the sorption sites occupied by the carbon dioxide. Moreover, it is the best replacement for shale oil and contributes more to the massive sequestration of carbon dioxide. When CO_2 is mixed with n-butane, n-octane, and n-dodecane in a 4 : 1 ratio, the difference in sorption between the components is large, and CO_2 does not have the same replacement capacity for different components

(3) The adsorption of carbon dioxide, n-butane, and n-octane in the organic matter nanopores of the multicomponent fluids first increased and then decreased with temperature, reaching a maximum at a temperature of 373 K. The adsorption of n-dodecane first decreased and then increased until the maximum adsorption of n-dodecane was reached at a temperature of 433 K

(4) The adsorption of carbon dioxide, n-butane, and n-octane by organic nanopores increases as the pore size increases. Meanwhile, the adsorption occupancy of n-dodecane in the competitive adsorption of multicomponent fluids first increases and then decreases. The larger the pore size, the lower the adsorption ratio. This is more conducive to the competitive adsorption between carbon dioxide and multicomponent fluids and the replacement of shale oil in shale storage by carbon dioxide

(5) The heat of adsorption is CO_2, $C_{12}H_{26}$, C_8H_{18}, and C_4H_{10} in descending order. As the temperature increases, the equivalent heat of adsorption of carbon dioxide, n-butane, and n-octane firstly increases and then decreases while that of n-dodecane firstly decreases and then increases. Moreover, there is a positive correlation between the adsorption amount of all four components in organic nanopores

Data Availability

All data included in this study are available upon request by contact with the corresponding author.

Conflicts of Interest

The authors declare no conflicts of interest.

Acknowledgments

The authors would like to appreciate the financial support of the National Natural Science Foundation of China [No. 52004038], funding name: Study on the Microscopic Phase Behavior and Migration Mechanism of CO2 and Multicomponent Alkanes in Shale Dynamical Nanopore. The authors also would like to appreciate the support of the General Project of Natural Science Research in Colleges and Universities of Jiangsu Province [No. 20KJB440003], study on carbon dioxide-methane transport mechanism of coal seam nanopores with multiple inducement deformation fields.

References

[1] X. H. Chen, "Research progress of shale oil reservoir state and resource evaluation methods," *Science Technology and Engineering*, vol. 17, no. 3, pp. 136–144, 2017.

[2] W. Dang, S. Jiang, J. Zhang et al., "A systematic experimental and modeling study of water adsorption/desorption behavior in organic-rich shale with different particle sizes," *Chemical Engineering Journal*, vol. 426, p. 130596, 2021.

[3] M. M. Guo, "Molecular simulation study of adsorption and flow characteristics of tight oil," *China University of Petroleum (East China)*, pp. 8–16, 2018.

[4] X. Yang, S. Liu, J. S. Le Zhang, and T. Ye, "Design and analysis of a renewable energy power system for shale oil exploitation using hierarchical optimization," *Energy*, vol. 206, p. 118078, 2020.

[5] B. Dai, E. D. Li, and X. J. Wang, "Evaluation of shale oil transport and accumulation patterns based on hydrocarbon geochemical parameters," *Oil and gas reservoir*, vol. 11, no. 4, pp. 506–513, 2021.

[6] M. Lin, W. B. Jiang, and Y. Li, "Some issues in the micro-scale flow of shale oil (gas)," *Mineral and Rock Geochemistry Bulletin*, vol. 34, no. 1, pp. 18–28, 2015.

[7] Y. Shu, D. Hassan, and B. Mojtaba, "A molecular dynamics explanation for fast imbibition of oil in organic tight rocks," *Fuel*, vol. 190, pp. 409–419, 2017.

[8] N. Li, B. Ding, Z. K. Gu, and L. Gong, "Molecular simulation of competing gas adsorption properties within different composite shale models," *Thermal Science and Technology*, vol. 20, no. 4, pp. 380–385, 2021.

[9] B. Zhang, T. H. Kang, and J. T. Kang, "Molecular simulation of competitive adsorption of C_2H_6, CH_4 on kaolinite surface," *Journal of Taiyuan University of Technology*, vol. 50, no. 3, pp. 297–302, 2019.

[10] F. Guo, S. Wang, Q. Feng, X. Yao, Q. Xue, and X. Li, "Adsorption and absorption of supercritical methane within shale kerogen slit," *Journal of Molecular Liquids*, vol. 320, p. 114364, 2020.

[11] Z. Cao, H. Jiang, J. Zeng et al., "Nanoscale liquid hydrocarbon adsorption on clay minerals: a molecular dynamics simulation of shale oils," *Chemical Engineering Journal*, vol. 420, p. 127578, 2021.

[12] Y. Yang, J. Liu, J. Yao et al., "Adsorption behaviors of shale oil in kerogen slit by molecular simulation," *Chemical Engineering Journal*, vol. 387, p. 124054, 2020.

[13] M. Pathak, G. Pawar, H. Huang, and M. D. Deo, "Carbon dioxide sequestration and hydrocarbons recovery in the gas rich shales: an insight from the molecular dynamics simulations," *Carbon Management Technology Conference*, pp. 1–5, 2015.

[14] Z. Q. Wu and Z. P. Liu, "Monte Carlo simulation of CO/H_2 adsorption and separation in carbon nano slits," *Journal of Beijing University of Chemical Technology (Natural Science Edition)*, vol. 36, no. 4, pp. 1–6, 2009.

[15] J. P. Zhou, X. F. Xia, and X. H. Li, "Molecular simulation of CO_2/CH_4 competitive adsorption in slit-type pores," *Journal of Coal*, vol. 35, no. 9, pp. 1512–1517, 2010.

[16] G. Chen, J. Zhang, S. Lu et al., "Adsorption behavior of hydrocarbon on Illite," *Energy & Fuels*, vol. 30, no. 11, pp. 9114–9121, 2016.

[17] S. Wang, Q. Feng, M. Zha et al., "Molecular dynamics simulation of liquid alkane occurrence state in pores and slits of shale organic matter," *Petroleum Exploration and Development*, vol. 42, no. 6, pp. 844–851, 2015.

[18] C. Wang, "Molecular dynamics simulation study on the micro mechanism of supercritical carbon dioxide replacement shale oil," *China University of Petroleum (East China)*, pp. 15–28, 2017.

[19] C. F. Zhu, M. Z. Dong, and H. J. Gong, "Competitive adsorption behaviors of carbon dioxide and n-dodecane mixtures in 13X molecular sieve," *IOP Conference Series: Earth and Environmental Science*, vol. 108, no. 2, p. 022079, 2018.

[20] Q. G. Li, C. H. Nie, and H. M. Zhang, "Application of molecular simulation in structural optimization and catalysis of molecular sieves," *Chemical Engineer*, vol. 31, no. 3, pp. 51–55, 2017.

[21] D. L. Bish and R. B. Von Dreele, "Rietveld refinement of non-hydrogen atomic positions in kaolinite," *Clays and Clay Minerals*, vol. 37, no. 4, pp. 289–296, 1989.

[22] R. R. Qi, *Study on the Mechanism of Multi-Component Competitive Adsorption of Shale Gas*, China University of Petroleum (Beijing), 2019.

[23] D. F. Zhang, Y. J. Cui, and S. G. Li, "Adsorption-diffusion behavior of methane and carbon dioxide in different coal rank coals," *Journal of Coal*, vol. 36, no. 10, pp. 1693–1698, 2011.

[24] C. Z. Wu, H. T. Xue, and S. F. Lu, "Molecular dynamics simulation of shale oil adsorption characteristics in nanoscale slits," *Geological Science and Technology Information*, vol. 37, no. 3, pp. 202–209, 2018.

[25] F. Xiong, G. Rother, D. Tomasko, W. Pang, and J. Moortgat, "On the pressure and temperature dependence of adsorption densities and other thermodynamic properties in gas shales," *Chemical Engineering Journal*, vol. 395, p. 124989, 2020.

[26] S. Fakher and O. Imqam, "Application of carbon dioxide injection in shale oil reservoirs for increasing oil recovery and carbon dioxide storage," *Fuel*, vol. 265, p. 116944, 2020.

[27] X. Zhou, G. Yang, and T. Yi, "Relationship between shale adsorption capacity and temperature and comparison of adsorption models," *Journal of Chongqing Institute of Science and Technology (Natural Science Edition)*, vol. 21, no. 1, 2019.

[28] B. H. Wang, Q. Yan, and W. L. Qiang, "Molecular dynamics simulation of the interfacial behavior of the C_ (12) E_2-n-dodecane-water system," *Henan Chemical Industry*, vol. 35, no. 3, pp. 23–26, 2018.

[29] I. Suárez-Ruiz, T. Juliao, F. Suárez-García, R. Marquez, and B. Ruiz, "Porosity development and the influence of pore size on the CH4 adsorption capacity of a shale oil reservoir (Upper Cretaceous) from Colombia. Role of solid bitumen," *International Journal of Coal Geology*, vol. 159, pp. 1–17, 2016.

[30] H. Q. Xue, H. Y. Wang, and H. L. Liu, "Adsorption properties and pore structure characteristics of shale - an example of Longmaxi Formation shale in Sichuan Basin," *Journal of Petroleum*, vol. 34, no. 5, pp. 826–832, 2013.

[31] L. Gao and J. Li, "A decoupled stabilized finite element method for thedual-porosity-Navier–Stokesfluid flow model arising in shale oil," *Numerical Methods for Partial Differential Equations*, vol. 37, no. 3, pp. 2357–2374, 2021.

[32] S. Zhou, H. Wang, P. Zhang, and W. Guo, "Investigation of the isosteric heat of adsorption for supercritical methane on shale under high pressure," *Adsorption Science & Technology*, vol. 37, no. 7-8, pp. 590–606, 2019.